SCIENCE CHINA
Information Sciences

• RESEARCH PAPER •

August 2026, Vol. 69, Iss. 8, 182201:1–182201:13
https://doi.org/10.1007/s11432-025-4944-8

Bearing-only circumnavigation with vector estimator using a fully actuated system approach

Shida CAO[1] & Guangren DUAN[1,2*]

[1]*Center for Control Theory and Guidance Technology, Harbin Institute of Technology, Harbin 150001, China*
[2]*Shenzhen Key Laboratory of Control Theory and Intelligent Systems, Southern University of Science and Technology, Shenzhen 518055, China*

Received 8 March 2025/Revised 16 June 2025/Accepted 10 August 2025/Published online 31 July 2026

Abstract This study investigates the bearing-only circumnavigation (BOC) problem involving the control of agent acceleration to encircle static and moving targets at a prescribed distance and tangential speed. The agent obtains navigation information by measuring its position and velocity. However, the agent only measures the bearing angle from the agent to the target to obtain information about the target, since the position of the target is unmeasurable. To estimate the unknown position of the target, we adopt Deghats vector estimator, the convergence of which relies on a persistent excitation condition. By modeling the dynamics of this problem as a fully actuated system (FAS), we apply a novel, flourishing FAS-approach-based control method to solve this acceleration-design BOC problem. For the static target case, we design an FAS-based controller and prove the stability of the closed-loop system. For the moving target case, we design a robust FAS-based controller and prove the boundedness property of the closed-loop system. Three simulations are conducted across noiseless static, noisy static, and moving target cases to verify the feasibility of the proposed control methods.

Keywords fully actuated system approach, multi-agent systems, bearing-only circumnavigation, vector estimator, acceleration controller

Citation Cao S D, Duan G R. Bearing-only circumnavigation with vector estimator using a fully actuated system approach. Sci China Inf Sci, 2026, 69(8): 182201, https://doi.org/10.1007/s11432-025-4944-8

1 Introduction

Bearing-only circumnavigation (BOC) is a crucial problem within multi-agent system circumnavigation control research. In circumnavigation problems, agents need to encircle a target to perform various tasks, including security surveillance, search & rescue, exploration, source seeking, and military operations. Several studies have explored different types of circumnavigation problems based on unique operating conditions, such as incomplete information circumnavigation problems, which include the distance-only circumnavigation problem and the BOC problem. In the BOC problem, agents only measure the direction from themselves to the target. The advantages of the BOC setting include the following.

- Fewer sensors at lower cost.
- The possibility of being deployed in distance sensor failure scenarios.
- Applicability in radio silence scenarios.

In 2010, Deghat's classic study [1] proposed the BOC problem, solving a problem involving an agent and a target. Ever since, approximately 70 publications have explored BOC problems, with notable representative studies [1–26].

The fully actuated system (FAS) approach is new within the control research domain. In 2020, Duan proposed the FAS theory [27–29], demonstrating that FASs exist across a wide range and that the FAS approach is a highly effective method for nonlinear systems. Refs. [27, 28] revealed that many real-world control systems can be simulated as mathematical FASs despite being under-actuated. Ref. [30] explored uncertain FAS models, leveraging the Lyapunov stability theory to demonstrate a direct approach for designing robust stabilizing controllers for these uncertain FAS models. Ref. [31] proposed mixed-order FASs for general control systems, demonstrating the possibility of representing a general control system using a controllable subsystem described by an FAS model and an extra uncontrollable or supplementary subsystem.

However, the acceleration design problem has been rarely studied among established BOC problems. As FAS approaches are highly effective for high-order control systems owing to their capability of facilitating arbitrary pole

* Corresponding author (email: g.r.duan@hit.edu.cn)

configuration after nonlinear cancellation, they can be applied to solve the second-order acceleration-design BOC problem. The first FAS-based BOC study [23] identified the BOC problem as a unique FAS problem with distinct features. For instance, the immeasurable nature of the first state necessitates the integration of estimation methods. Consequently, the FAS approach is crucial to BOC research, making the BOC problem a specialized case within the FAS research domain.

To estimate the unknown position of the target, implementing an estimator is essential for BOC problems. There are two types of estimators.

The vector estimator was proposed by Deghat et al. [1]. This estimator represents a valuable technical roadmap in the BOC research domain, with numerous representative studies [2–4, 7, 10, 14, 15, 17].

The scalar estimator was proposed by [13]. This estimator was proposed for safety purposes and has been applied in several studies [16, 23, 25].

Compared with the scalar estimator, the vector estimator does not utilize explicit measurement derivatives. Thus, it is more resistant to high-frequency noise. Ref. [23] adopted the scalar estimator to solve the BOC problem via the FAS approach. Considering the advantage of the vector estimator, a logical move is to replace the scalar estimator of [23] with a vector alternative. However, this transition introduces technical challenges owing to the fundamentally different convergence conditions required by the two estimators. In this study, we solve the BOC problem based on the FAS framework integrated with the vector estimator. We consider static and moving target cases. Given that the FAS-based BOC research is at its early stages, we investigate the most classic case involving only an agent and a target. Consistent with the existing literature on vector estimators, we also analyze the persistent excitation (PE) property. In the static target case, we prove that the PE condition is satisfied during the circumnavigation process. For the moving target case, the PE condition is guaranteed via specific robust control design tools. The contributions of this study are summarized below.

(1) Compared with [23], the vector estimator is used, enhancing the resistance of the BOC control system to high-frequency noise. We extend the vector estimator to the acceleration controller design problem. This demonstrates the crucial effect of the FAS theory [28] for BOC control problems. Since the FAS framework simplifies the controller design by decoupling dynamics, we introduce a novel approach to address the acceleration-design BOC problem.

(2) A FAS-based acceleration controller is designed for the static target case. We prove that the closed-loop system influenced by this controller and the vector estimator is stable. By modeling the BOC system as a mixed-order FAS, we simplify the controller design, allowing us to assign the poles. This study demonstrates the relevance of the FAS theory [31] in stabilizing BOC control.

(3) We design a FAS-based robust acceleration controller for moving target cases. This controller enables us to prove the boundedness of the closed-loop system state. The FAS structure offers a convenient design framework for robust controllers [30], demonstrating the criticality of the FAS robust theory for addressing the BOC control problem for moving targets.

The remainder of the paper is structured as follows. Section 2 presents the BOC problem and the vector estimator as well as the system model. The static target case is analyzed in Section 3. Here, the mixed-order FAS controller is designed to stabilize the BOC system. Section 4 investigates the moving target case by designing the FAS robust controller and proving the boundedness property. Section 5 validates the method via three simulations: the noiseless static, noisy static, and the moving target cases. Section 6 concludes the study and offers some meaningful directions for future studies.

The following notations are used.

$\mathbb{R}$: set of real numbers.

$\mathbb{R}_+$: set of positive real numbers.

$\mathbb{R}_{\geqslant 0}$: set of nonnegative real numbers.

$\mathbb{R}^n$: set of n-dimensional column vectors.

$\mathbb{R}^{m\times n}$: set of $m \times n$ matrices.

$\mathbb{S}^1$: set of two-dimensional unit column vectors.

$\mathbf{0}$: origin of $\mathbb{R}^2$.

$\boldsymbol{I}$: 2×2 identity matrix.

$\|\cdot\|$: vector 2-norm.

Unless defined for the first time, we typically omit the dependence of variables on the time t, e.g., $a = a(t)$.

2 Problem statement and model construction

In this section, the most basic BOC problem, namely, the single-agent single-target case, is comprehensively introduced. Thereafter, the vector estimator for our controller design is proposed.

2.1 Bearing-only circumnavigation problem

We present the single-agent single-target BOC problem.

Our system comprises only one agent and one target, and both the static and the moving target cases are studied. The velocity of the target is unknown in the moving target case, and the acceleration of the agent is controlled. The control objective of this circumnavigation problem is to ensure that the agent orbits the target with a desired distance and tangential speed. Our BOC problem is unique in that only the bearing information of the target, i.e., the directional measurement, is measurable. The range information of the target, i.e., the distance measurement, is not directly measurable by the agent. Regarding other known information, some navigation information of the agent is known, namely, its position and velocity.

For readers' convenience, we shall first outline the basic variables employed in our BOC problem.

$\boldsymbol{x}(t) \in \mathbb{R}^2$: position of target.

$\boldsymbol{y}(t) \in \mathbb{R}^2$: position of agent.

$\rho(t) \in \mathbb{R}_{\geqslant 0}$: agent-target distance, $\rho = \|\boldsymbol{x} - \boldsymbol{y}\|$.

$d \in \mathbb{R}_+$: desired agent-target distance.

$\alpha \in \mathbb{R}_+$: desired tangential speed of agent.

Subsequently, we introduce the relevant variables to the bearing information. Mathematically, the bearing information is represented by radial and tangential unit vectors $\boldsymbol{\varphi}$, $\bar{\boldsymbol{\varphi}}$ of the agent relative to the target.

$\boldsymbol{\varphi}(t) \in \mathbb{S}^1$: bearing information, radial unit vector, $\boldsymbol{\varphi} = (\boldsymbol{x} - \boldsymbol{y})/\rho$.

$\bar{\boldsymbol{\varphi}}(t) \in \mathbb{S}^1$: bearing information, $\bar{\boldsymbol{\varphi}}$ obtained via a 90° clockwise rotation of $\boldsymbol{\varphi}$.

$v(t) \in \mathbb{R}$: radial speed of the agent, $v = \boldsymbol{\varphi}^{\mathrm{T}}\dot{\boldsymbol{y}}$.

$\bar{v}(t) \in \mathbb{R}$: tangential speed of the agent, $\bar{v} = \bar{\boldsymbol{\varphi}}^{\mathrm{T}}\dot{\boldsymbol{y}}$.

$\omega(t) \in \mathbb{R}$: angular speed of the agent, $\omega = \bar{v}/\rho$.

$v_x(t) \in \mathbb{R}$: speed of the target along $\boldsymbol{\varphi}$, $v_x = \boldsymbol{\varphi}^{\mathrm{T}}\dot{\boldsymbol{x}}$.

$\bar{v}_x(t) \in \mathbb{R}$: speed of the target along $\bar{\boldsymbol{\varphi}}$, $\bar{v}_x = \bar{\boldsymbol{\varphi}}^{\mathrm{T}}\dot{\boldsymbol{x}}$.

$a_x(t) \in \mathbb{R}$: acceleration of the target along $\boldsymbol{\varphi}$, $a_x = \boldsymbol{\varphi}^{\mathrm{T}}\ddot{\boldsymbol{x}}$.

2.2 Vector estimator

The vector estimator is described in this subsection.

The challenge of our BOC problem lies in the fact that the position of the target is not directly measurable. Since this position is unknown, something must be designed for its estimation. Thus, we employ the vector estimator proposed by Deghat et al. [1], as widely referenced in BOC studies. If the readers want to learn another estimator—the scalar estimator—please refer to [13, 16, 25].

Variables for estimating the position of the target are introduced as follows.

$\hat{\boldsymbol{x}}(t) \in \mathbb{R}^2$: estimated position of the target.

$\hat{\rho}(t) \in \mathbb{R}$: estimated agent-target distance along $\boldsymbol{\varphi}$, $\hat{\rho} = \boldsymbol{\varphi}^{\mathrm{T}}(\hat{\boldsymbol{x}} - \boldsymbol{y})$.

Remark 1. Our definition of $\hat{\rho}$ differs from that of [13]. The estimated agent-target distance $\hat{\rho}$ is obtained based on the estimated position of the target $\hat{\boldsymbol{x}}$. Thus, the position of the target $\boldsymbol{x}$ is first estimated, followed by $\hat{\boldsymbol{x}}$. This approach differs from [13] where the agent-target distance ρ is first estimated, followed by $\hat{\rho}$.

Our adopted vector estimator [1] is given by the following:

$$\dot{\hat{\boldsymbol{x}}} = k\bar{\boldsymbol{\varphi}}\bar{\boldsymbol{\varphi}}^{\mathrm{T}}(\boldsymbol{y} - \hat{\boldsymbol{x}}), \tag{1}$$

where $k \in \mathbb{R}_+$ is a coefficient. Notably, $\bar{\boldsymbol{\varphi}}\bar{\boldsymbol{\varphi}}^{\mathrm{T}}$ is an orthogonal projection matrix that projects vectors onto the $\bar{\boldsymbol{\varphi}}$ direction along $\boldsymbol{\varphi}$. This estimator is described in Figure 1. The derivative $\dot{\hat{\boldsymbol{x}}}$ indicates the line passing $\boldsymbol{x}$ and the position of the agent $\boldsymbol{y}$. This indicates that $\hat{\boldsymbol{x}}$ converges tangentially.

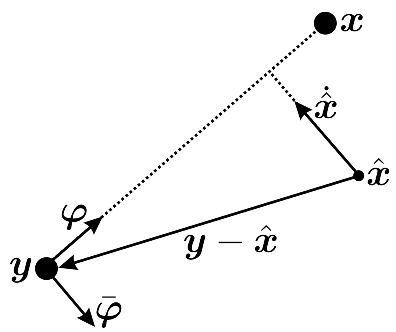

Figure 1 Description of the vector estimator.

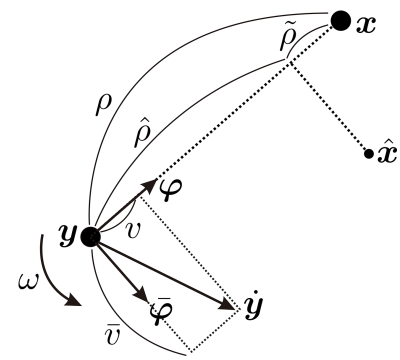

Figure 2 Description of variables.

2.3 Problem statement

In this subsection, we provide a formal statement for our BOC problem.

The error notations are described as follows.

$e_\rho(t) \in \mathbb{R}$: agent-target distance error, $e_\rho = \rho - d$.

$e_{\bar{\upsilon}}(t) \in \mathbb{R}$: tangential speed error, $e_{\bar{\upsilon}} = \bar{\upsilon} - \alpha$.

$\tilde{\boldsymbol{x}} \in \mathbb{R}^2$: estimation error of target's position, $\tilde{\boldsymbol{x}} = \boldsymbol{x} - \hat{\boldsymbol{x}}$.

$\tilde{\rho}(t) \in \mathbb{R}$: estimation error of the agent-target distance, $\tilde{\rho} = \rho - \hat{\rho}$.

$\hat{e}_\rho(t) \in \mathbb{R}$: estimated error of the agent C target distance, $\hat{e}_\rho = \hat{\rho} - d$.

Remark 2. Our definition of the estimation error of the position of the target, $\tilde{\boldsymbol{x}}$, differs from that of [1], where $\tilde{\boldsymbol{x}}$ is defined as $\hat{\boldsymbol{x}} - \boldsymbol{x}$.

Thus far, all the basic variables in our BOC problem have been introduced, and the main variables are illustrated in Figure 2.

Next, we formally describe our BOC problem. In the static target case, the BOC problem is a stabilization control problem.

Problem 1 (Static target case). Given the knowledge of the agent's position $\boldsymbol{y}$, the agent's velocity $\dot{\boldsymbol{y}}$, the agent's angular speed ω, the radial unit vector $\boldsymbol{\varphi}$, the tangential unit vector $\bar{\boldsymbol{\varphi}}$, and using the vector estimator (1), design the agent's acceleration $\ddot{\boldsymbol{y}}$ such that$\lim_{t\to\infty} e_\rho(t) = 0$, $\lim_{t\to\infty} e_{\bar{\upsilon}}(t) = 0$.

In the moving target case, the unknown velocity of the target introduces uncertainty to the BOC problem, making it a robust control problem; moreover, our control objective focuses on the boundedness property.

Problem 2 (Moving target case). Given the knowledge of the agent's position $\boldsymbol{y}$, the agent's velocity $\dot{\boldsymbol{y}}$, the agent's angular speed ω, the radial unit vector $\boldsymbol{\varphi}$, the tangential unit vector $\bar{\boldsymbol{\varphi}}$, and using the vector estimator (1), design the agent's acceleration $\ddot{\boldsymbol{y}}$ such that

(1) the agent-target distance error e_ρ, the agent's tangential speed error $e_{\bar{\upsilon}}$, and the target's position estimation error $\tilde{\boldsymbol{x}}$ are bounded;

(2) the agent's tangential speed $\bar{\upsilon}$ keeps positive.

Remark 3. In the second item, $\bar{\upsilon}$ ensures that the circling movement is performed while guaranteeing the boundedness property in the first item.

2.4 Construction of the FAS model

Here, we obtain the estimation error dynamics, (2), and derive the mixed-order FAS model.

First, we study (1), revealing that Eq. (2) of the position of the target is given as follows:

$$\begin{aligned}\dot{\tilde{\boldsymbol{x}}} &= \dot{\boldsymbol{x}} - \dot{\hat{\boldsymbol{x}}} = -k\bar{\boldsymbol{\varphi}}\bar{\boldsymbol{\varphi}}^{\mathrm{T}}(\boldsymbol{y} - \hat{\boldsymbol{x}}) + \dot{\boldsymbol{x}} = -k\bar{\boldsymbol{\varphi}}\bar{\boldsymbol{\varphi}}^{\mathrm{T}}[(\boldsymbol{y} - \boldsymbol{x}) + (\boldsymbol{x} - \hat{\boldsymbol{x}})] + \dot{\boldsymbol{x}} \\ &= -k\bar{\boldsymbol{\varphi}}\bar{\boldsymbol{\varphi}}^{\mathrm{T}}(\boldsymbol{x} - \hat{\boldsymbol{x}}) + \dot{\boldsymbol{x}} = -k\bar{\boldsymbol{\varphi}}\bar{\boldsymbol{\varphi}}^{\mathrm{T}}\tilde{\boldsymbol{x}} + \dot{\boldsymbol{x}}.\end{aligned} \tag{2}$$

Moreover, the relation between the estimation error of the agent-target distance, $\tilde{\rho}$, and the estimation error of the position of the target, $\tilde{\boldsymbol{x}}$, is given as follows:

$$\tilde{\rho} = \rho - \hat{\rho} = \boldsymbol{\varphi}^{\mathrm{T}}(\boldsymbol{x} - \boldsymbol{y}) - \boldsymbol{\varphi}^{\mathrm{T}}(\hat{\boldsymbol{x}} - \boldsymbol{y}) = \boldsymbol{\varphi}^{\mathrm{T}}(\boldsymbol{x} - \hat{\boldsymbol{x}}) = \boldsymbol{\varphi}^{\mathrm{T}}\tilde{\boldsymbol{x}}. \tag{3}$$

Second, we derive the mixed-order FAS model. Previous studies generally solve their BOC problems without an explicit system equation. However, we adopt the FAS approach to solve our acceleration-design BOC problem. In the FAS framework, a system equation must be explicitly defined. We select ρ and $\bar{v}$ as system variables. The derivative of ρ is

$$\dot{\rho} = \frac{\mathrm{d}}{\mathrm{d}t}\|\boldsymbol{x} - \boldsymbol{y}\| = \frac{(\boldsymbol{x} - \boldsymbol{y})^{\mathrm{T}}(\dot{\boldsymbol{x}} - \dot{\boldsymbol{y}})}{\rho} = \boldsymbol{\varphi}^{\mathrm{T}}(\dot{\boldsymbol{x}} - \dot{\boldsymbol{y}}) \tag{4a}$$

$$= \boldsymbol{\varphi}^{\mathrm{T}}\dot{\boldsymbol{x}} - \boldsymbol{\varphi}^{\mathrm{T}}\dot{\boldsymbol{y}} = v_x - v. \tag{4b}$$

By noting that $\boldsymbol{I} = \boldsymbol{\varphi}\boldsymbol{\varphi}^{\mathrm{T}} + \bar{\boldsymbol{\varphi}}\bar{\boldsymbol{\varphi}}^{\mathrm{T}}$, with (4a), we derive

$$\dot{\boldsymbol{\varphi}} = \frac{\mathrm{d}}{\mathrm{d}t}\frac{\boldsymbol{x} - \boldsymbol{y}}{\rho} = \frac{\rho(\dot{\boldsymbol{x}} - \dot{\boldsymbol{y}}) - \dot{\rho}(\boldsymbol{x} - \boldsymbol{y})}{\rho^2} = \frac{\dot{\boldsymbol{x}} - \dot{\boldsymbol{y}} - \dot{\rho}\boldsymbol{\varphi}}{\rho} = \frac{\dot{\boldsymbol{x}} - \dot{\boldsymbol{y}} - \boldsymbol{\varphi}\boldsymbol{\varphi}^{\mathrm{T}}(\dot{\boldsymbol{x}} - \dot{\boldsymbol{y}})}{\rho} = \frac{(\boldsymbol{I} - \boldsymbol{\varphi}\boldsymbol{\varphi}^{\mathrm{T}})(\dot{\boldsymbol{x}} - \dot{\boldsymbol{y}})}{\rho}$$
$$= \frac{\bar{\boldsymbol{\varphi}}\bar{\boldsymbol{\varphi}}^{\mathrm{T}}(\dot{\boldsymbol{x}} - \dot{\boldsymbol{y}})}{\rho} = \frac{\bar{\boldsymbol{\varphi}}^{\mathrm{T}}\dot{\boldsymbol{x}} - \bar{\boldsymbol{\varphi}}^{\mathrm{T}}\dot{\boldsymbol{y}}}{\rho}\bar{\boldsymbol{\varphi}} = \frac{\bar{v}_x - \bar{v}}{\rho}\bar{\boldsymbol{\varphi}} = \left(\frac{\bar{v}_x}{\rho} - \omega\right)\bar{\boldsymbol{\varphi}}.$$

Thereafter,

$$\dot{\bar{\boldsymbol{\varphi}}} = \frac{\mathrm{d}}{\mathrm{d}t}\left(\begin{bmatrix} 0 & 1 \\ -1 & 0 \end{bmatrix}\boldsymbol{\varphi}\right) = \begin{bmatrix} 0 & 1 \\ -1 & 0 \end{bmatrix}\dot{\boldsymbol{\varphi}} = \left(\frac{\bar{v}_x}{\rho} - \omega\right)\begin{bmatrix} 0 & 1 \\ -1 & 0 \end{bmatrix}\bar{\boldsymbol{\varphi}} = \left(\frac{\bar{v}_x}{\rho} - \omega\right)(-\boldsymbol{\varphi}) = \left(\omega - \frac{\bar{v}_x}{\rho}\right)\boldsymbol{\varphi}.$$

Hence, we know that

$$\dot{\boldsymbol{\varphi}} = \left(\frac{\bar{v}_x}{\rho} - \omega\right)\bar{\boldsymbol{\varphi}}, \tag{5}$$

$$\dot{\bar{\boldsymbol{\varphi}}} = \left(\omega - \frac{\bar{v}_x}{\rho}\right)\boldsymbol{\varphi}. \tag{6}$$

With (4a) and (5), taking the derivative of $\dot{\rho}$ yields

$$\ddot{\rho} = \frac{\mathrm{d}}{\mathrm{d}t}[\boldsymbol{\varphi}^{\mathrm{T}}(\dot{\boldsymbol{x}} - \dot{\boldsymbol{y}})] = \dot{\boldsymbol{\varphi}}^{\mathrm{T}}(\dot{\boldsymbol{x}} - \dot{\boldsymbol{y}}) + \boldsymbol{\varphi}^{\mathrm{T}}(\ddot{\boldsymbol{x}} - \ddot{\boldsymbol{y}}) = \left(\frac{\bar{v}_x}{\rho} - \omega\right)\bar{\boldsymbol{\varphi}}^{\mathrm{T}}(\dot{\boldsymbol{x}} - \dot{\boldsymbol{y}}) + \boldsymbol{\varphi}^{\mathrm{T}}(\ddot{\boldsymbol{x}} - \ddot{\boldsymbol{y}})$$
$$= \left(\frac{\bar{v}_x}{\rho} - \omega\right)(\bar{v}_x - \bar{v}) + a_x - \boldsymbol{\varphi}^{\mathrm{T}}\ddot{\boldsymbol{y}} = \frac{\bar{v}_x^2}{\rho} - 2\bar{v}_x\omega + a_x + \bar{v}\omega - \boldsymbol{\varphi}^{\mathrm{T}}\ddot{\boldsymbol{y}}. \tag{7}$$

With (6), taking the derivative of $\bar{v}$ yields

$$\dot{\bar{v}} = \frac{\mathrm{d}}{\mathrm{d}t}(\bar{\boldsymbol{\varphi}}^{\mathrm{T}}\dot{\boldsymbol{y}}) = \dot{\bar{\boldsymbol{\varphi}}}^{\mathrm{T}}\dot{\boldsymbol{y}} + \bar{\boldsymbol{\varphi}}^{\mathrm{T}}\ddot{\boldsymbol{y}} = \left(\omega - \frac{\bar{v}_x}{\rho}\right)\boldsymbol{\varphi}^{\mathrm{T}}\dot{\boldsymbol{y}} + \bar{\boldsymbol{\varphi}}^{\mathrm{T}}\ddot{\boldsymbol{y}}$$
$$= \left(\omega - \frac{\bar{v}_x}{\rho}\right)v + \bar{\boldsymbol{\varphi}}^{\mathrm{T}}\ddot{\boldsymbol{y}} = -\frac{v\bar{v}_x}{\rho} + v\omega + \bar{\boldsymbol{\varphi}}^{\mathrm{T}}\ddot{\boldsymbol{y}}. \tag{8}$$

Combining (7) and (8) yields the following system equation:

$$\begin{cases} \ddot{\rho} = \dfrac{\bar{v}_x^2}{\rho} - 2\bar{v}_x\omega + a_x + \bar{v}\omega - \boldsymbol{\varphi}^{\mathrm{T}}\ddot{\boldsymbol{y}}, \\ \dot{\bar{v}} = -\dfrac{v\bar{v}_x}{\rho} + v\omega + \bar{\boldsymbol{\varphi}}^{\mathrm{T}}\ddot{\boldsymbol{y}}. \end{cases}$$

Denoting that

$$\boldsymbol{f}(t) = \begin{bmatrix} \dfrac{[\bar{v}_x(t)]^2}{\rho(t)} - 2\bar{v}_x(t)\omega(t) + a_x(t) + \bar{v}(t)\omega(t) \\ -\dfrac{v(t)\bar{v}_x(t)}{\rho(t)} + v(t)\omega(t) \end{bmatrix}, \quad \boldsymbol{B}(t) = \begin{bmatrix} -[\boldsymbol{\varphi}(t)]^{\mathrm{T}} \\ [\bar{\boldsymbol{\varphi}}(t)]^{\mathrm{T}} \end{bmatrix},$$

thereafter, the error system equation is given as follows:

$$\begin{bmatrix} \ddot{e}_{\rho} \\ \dot{e}_{\bar{v}} \end{bmatrix} = \boldsymbol{f} + \boldsymbol{B}\ddot{\boldsymbol{y}}. \tag{9}$$

Notably, $\det(\boldsymbol{B}) = 1 \neq 0$ or ∞. Hence, the error system (9), is obtained as a mixed-order FAS [31].

3 Static target case

The static target case is explored in this section. First, we propose the FAS controller, after which we prove the asymptotic stability of the closed-loop system.

3.1 Design of the FAS controller

We design the FAS controller of the static target case and present the assumptions.

We define

$$\boldsymbol{f}_0(t) = \begin{bmatrix} \bar{v}(t)\omega(t) \\ v(t)\omega(t) \end{bmatrix}.$$

Next, we substitute $\dot{\boldsymbol{x}} = \boldsymbol{0}$ into (9) and (2) to obtain

$$\begin{bmatrix} \ddot{e}_\rho \\ \dot{e}_{\bar{v}} \end{bmatrix} = \boldsymbol{f}_0 + \boldsymbol{B}\ddot{\boldsymbol{y}} \tag{10}$$

and

$$\dot{\tilde{\boldsymbol{x}}} = -k\bar{\boldsymbol{\varphi}}\bar{\boldsymbol{\varphi}}^{\mathrm{T}}\tilde{\boldsymbol{x}}. \tag{11}$$

The above represents the error system equation in the static target case. Based on the FAS theory, the controller is designed as follows:

$$\ddot{\boldsymbol{y}} = -\boldsymbol{B}^{-1}\left(\boldsymbol{f}_0 + \begin{bmatrix} -a_\rho^1 v + a_\rho^0 \hat{e}_\rho \\ a_{\bar{v}} e_{\bar{v}} \end{bmatrix}\right), \tag{12}$$

where a_ρ^1, a_ρ^0, and $a_{\bar{v}} \in \mathbb{R}$ are control coefficients. Notably, e_ρ is unknown; thus, we substitute it with $\hat{e}_\rho$. In the next subsection, we prove that this substitution does not influence convergence.

Next, we introduce the following assumption, which is a constraint for the control coefficients to guarantee stability.

Assumption 1. $a_\rho^1, a_\rho^0, a_{\bar{v}} \in \mathbb{R}_+$.

3.2 Stability analysis

Here, the asymptotic stability of the closed-loop system is proven.

Substituting the controller (12) into (9) yields the closed-loop error system equation:

$$\begin{cases} \ddot{e}_\rho + a_\rho^1 \dot{e}_\rho + a_\rho^0 e_\rho = a_\rho^0 \tilde{\rho}, & \text{(13a)} \\ \dot{e}_{\bar{v}} + a_{\bar{v}} e_{\bar{v}} = 0. & \text{(13b)} \end{cases}$$

First, the upper bound property of ρ is presented.

Lemma 1. Under Assumption 1, the vector estimator (1) and the controller (12), it follows that ρ is upper-bounded.

Proof. From (13a), we confirm

$$\ddot{\rho} + a_\rho^1 \dot{\rho} + a_\rho^0 \rho = a_\rho^1 d + a_\rho^0 \tilde{\rho}.$$

From Assumption 1 that $a_\rho^1, a_\rho^0 > 0$, we confirm that this is an input-state stable system. Assuming $\tilde{\rho}$ is bounded, we can immediately conclude that ρ is also bounded. Assuming $V = \tilde{\boldsymbol{x}}^{\mathrm{T}}\tilde{\boldsymbol{x}}/2$, Eq. (11) will yield

$$\dot{V} = \tilde{\boldsymbol{x}}^{\mathrm{T}}\dot{\tilde{\boldsymbol{x}}} = -k\tilde{\boldsymbol{x}}^{\mathrm{T}}\bar{\boldsymbol{\varphi}}\bar{\boldsymbol{\varphi}}^{\mathrm{T}}\tilde{\boldsymbol{x}} = -k(\bar{\boldsymbol{\varphi}}^{\mathrm{T}}\tilde{\boldsymbol{x}})^2 \leqslant 0.$$

Therefore, the boundedness of $\tilde{\boldsymbol{x}}$ is proven. From (3), we also confirm the boundedness of $\tilde{\rho}$, which indicates that ρ is also bounded. This concludes the proof.

Thereafter, the lower bound property of ω is proven.

Lemma 2. Under Assumption 1, the vector estimator (1) and the controller (12), it follows that after some time, ω exhibits a positive lower bound.

Proof. Note that $\omega = \bar{v}/\rho$. Lemma 1 confirms the upper-boundedness of ρ. Therefore, we only have to prove that $\bar{v}$ exhibits a positive lower bound after some time. Solving (13b) yields

$$e_{\bar{v}}(t) = e_{\bar{v}}(0)\exp(-a_{\bar{v}}t) = [\bar{v}(0) - \alpha]\exp(-a_{\bar{v}}t). \tag{14}$$

Hence,

$$\bar{v}(t) = e_{\bar{v}}(t) + \alpha = \alpha + [\bar{v}(0) - \alpha]\exp(-a_{\bar{v}}t) = \bar{v}(0)\exp(-a_{\bar{v}}t) + \alpha[1 - \exp(-a_{\bar{v}}t)] \to \alpha.$$

Thus, it is evident that $\bar{v}$ exhibits a positive lower bound after a certain time, concluding the proof.

For (11), the following well-known proposition is employed to prove the exponential convergence property of $\tilde{\boldsymbol{x}}$.

Proposition 1 (PE, [1, Proposition 1]). Let $V(t)\colon \mathbb{R}_{\geqslant 0} \to \mathbb{R}^{n\times r}$ be regulated. Subsequently, the linear time-varying system, $\dot{z}(t) = -V(t)V^{\mathrm{T}}(t)z(t)$, is exponentially and asymptotically stable if and only if for some positive α_1, α_2, and Δt; for all $t_0 \in \mathbb{R}_{\geqslant 0}$, there is

$$\alpha_1 I \leqslant \int_{t_0}^{t_0+\Delta t} V(t)V^{\mathrm{T}}(t)\,\mathrm{d}t \leqslant \alpha_2 I.$$

This condition is called the PE condition, and $V(t)$ is considered persistently exciting if it satisfies the above inequality. Another interpretation of the PE condition in scalar form is as follows:

$$\epsilon_1 \leqslant \int_{t_0}^{t_0+\Delta t} [U^{\mathrm{T}}V(t)]^2\,\mathrm{d}t \leqslant \epsilon_2, \quad \forall\, t_0 \in \mathbb{R}_{\geqslant 0},$$

where ϵ_1 and ϵ_2 are positive scalars, and $U \in \mathbb{R}^n$ can be any constant unit vector.

Now, the convergence of $\tilde{\rho}$ can be proven.

Lemma 3. Under Assumption 1, the vector estimator (1) and the controller (12), it follows that $\tilde{\rho}$ converges to zero.

Proof. Lemma 2 confirms that ω exhibits a positive lower bound after some time. Thus, $\bar{\boldsymbol{\varphi}}$ is persistently exciting. Employing Proposition 1, we determine that $\tilde{\rho}$ converges to zero, concluding the proof.

The lemma below proves the convergence of e_ρ.

Lemma 4. Consider the system $\ddot{z}(t) + a_1\dot{z}(t) + a_0 z(t) = f(t)$, where $z(t), f(t) \in \mathbb{R}$; $a_1, a_0 \in \mathbb{R}_+$. If $f(t)$ converges to zero, then $z(t)$ also converges to zero.

Proof. In the frequency domain, $z(s) = \frac{f(s)}{s^2+a_1 s+a_0}$. Since $f(t)$ converges to zero, as revealed by the final value theorem, we know that $\lim_{s\to 0} sf(s) = \lim_{t\to\infty} f(t) = 0$. Employing this theorem again, we confirm that $\lim_{t\to\infty} z(t) = \lim_{s\to 0} sz(s) = \lim_{s\to 0}\frac{sf(s)}{s^2+a_1 s+a_0} = \lim_{s\to 0}\frac{sf(s)}{a_0} = 0$. This concludes the proof.

Finally, we summarize our results in the following theorem, indicating the completion of the BOC task.

Theorem 1. Under Assumption 1, the vector estimator (1) and the controller (12), it follows that e_ρ and $e_{\bar{v}}$ converge to zero, solving Problem 1.

Proof. Based on Lemma 3, we confirm that $\tilde{\rho}$ converges to zero. Recalling (13a) and applying Lemma 4 reveals that e_ρ converges to zero. Employing (14), we confirm that $e_{\bar{v}}$ converges to zero, concluding the proof.

4 Moving target case

We investigate the moving target case. First, we design the FAS robust controller to solve this BOC problem. The boundedness properties of e_ρ and $e_{\bar{v}}$ are proven.

4.1 Design of a robust FAS controller

First, the constraint on the movement of the target is stated in the following assumption.

Assumption 2. For the velocity of the target, there exists $\varepsilon, \sigma \in \mathbb{R}_+$ such that $\|\dot{\boldsymbol{x}}(t)\| \leqslant \varepsilon$ and $\|\ddot{\boldsymbol{x}}(t)\| \leqslant \sigma$ for $t \geqslant 0$. Moreover, ε is known.

For the design of a robust controller, the following conjecture is crucial.

Conjecture 1. There exists a known value $\rho_* \in \mathbb{R}_+$, such that $\rho(t) \geqslant \rho_*$ for $t \geqslant 0$.

Remark 4. The value of the positive lower bound, ρ_*, is empirical. Usually, the ρ varies around the desired value d within a small range. In practice, we can adopt a sufficiently small value ρ_* for the controller design.

Here, Eq. (9) can be rewritten as follows:

$$\begin{bmatrix}\ddot{e}_\rho\\ \dot{e}_{\bar{v}}\end{bmatrix}=\begin{bmatrix}\bar{v}_x^2/\rho-2\bar{v}_x\omega+a_x\\ -v\bar{v}_x/\rho\end{bmatrix}+\boldsymbol{f}_0+\boldsymbol{B}\ddot{\boldsymbol{y}}. \tag{15}$$

The moving target case is more complicated than the static target case. When the target moves at a low velocity, the totally unknown velocity of the target makes the previous system a perturbed system.

Next, we design a robust FAS controller as follows:

$$\ddot{\boldsymbol{y}}=-\boldsymbol{B}^{-1}\left(\boldsymbol{f}_0+\begin{bmatrix}-a_\rho^1 v+a_\rho^0\hat{e}_\rho\\ a_{\bar{v}}e_{\bar{v}}+\dfrac{\varepsilon^2 e_{\bar{v}}v^2}{4\delta\rho_*^2}\end{bmatrix}\right). \tag{16}$$

Here, a_ρ^1, a_ρ^0, and $a_{\bar{v}}\in\mathbb{R}$ are control coefficients; $\delta\in\mathbb{R}_+$ is a design parameter that will be discussed below.

Remark 5. In the robust FAS controller (16), the terms $-a_\rho^1 v+a_\rho^0\hat{e}_\rho$ and $a_{\bar{v}}e_{\bar{v}}$ are pole assignment parts. Only the term, $\varepsilon^2 e_{\bar{v}}\boldsymbol{\zeta}^{\mathrm{T}}\boldsymbol{\zeta}/(4\delta\rho_*^2)$, is the robust part.

Substituting (16) into the error system (15), yields

$$\begin{cases}\ddot{e}_\rho-a_\rho^1 v+a_\rho^0\hat{e}_\rho=\dfrac{\bar{v}_x^2}{\rho}-2\bar{v}_x\omega+a_x,\\ \dot{e}_{\bar{v}}+a_{\bar{v}}e_{\bar{v}}+\dfrac{\varepsilon^2 e_{\bar{v}}v^2}{4\delta\rho_*^2}=-\dfrac{v\bar{v}_x}{\rho}.\end{cases}$$

Employing (4b), we confirm that the closed-loop error system equation is as follows:

$$\begin{cases}\ddot{e}_\rho+a_\rho^1\dot{e}_\rho+a_\rho^0 e_\rho=g, & \text{(17a)}\\ \dot{e}_{\bar{v}}+a_{\bar{v}}e_{\bar{v}}=-\dfrac{v\bar{v}_x}{\rho}-\dfrac{\varepsilon^2 e_{\bar{v}}v^2}{4\delta\rho_*^2}, & \text{(17b)}\end{cases}$$

where $g(t)=a_\rho^1 v_x(t)+a_\rho^0\tilde{\rho}(t)+\frac{[\bar{v}_x(t)]^2}{\rho(t)}-2\bar{v}_x(t)\omega(t)+a_x(t)$.

4.2 Boundedness of the tangential-speed error

In this subsection, we prove that $e_{\bar{v}}$ is bounded and that the bound can be arbitrarily regulated.

First, the following assumption is given.

Assumption 3. $a_{\bar{v}}\in\mathbb{R}_+$.

Thereafter, we report the following simple result.

Lemma 5. Let $a\in\mathbb{R}_+$, $b,c\in\mathbb{R}$. Thus, there holds $bc-ac^2\leqslant\frac{b^2}{4a}$.

Proof. It is evident that $bc-ac^2=-a\left(c-\frac{b}{2a}\right)^2+\frac{b^2}{4a}\leqslant\frac{b^2}{4a}$. This concludes the proof.

Thereafter, the boundedness property of $e_{\bar{v}}$ is stated below.

Lemma 6. Conjecture 1, Assumptions 2 and 3, (1), and (16) confirm the boundedness of $e_{\bar{v}}$.

Proof. Define the Lyapunov function, $V_{\bar{v}}=e_{\bar{v}}^2/2$. Assumption 2, Lemma 5, and Eq. (17b) yield the following:

$$\dot{V}_{\bar{v}}=e_{\bar{v}}\dot{e}_{\bar{v}}=-a_{\bar{v}}e_{\bar{v}}^2+\left(-\frac{\bar{v}_x}{\rho}\right)(ve_{\bar{v}})-\frac{\varepsilon^2}{4\delta\rho_*^2}(ve_{\bar{v}})^2\leqslant-a_{\bar{v}}e_{\bar{v}}^2+\delta\frac{\bar{v}_x^2}{\varepsilon^2}\frac{\rho_*^2}{\rho^2}\leqslant-2a_{\bar{v}}V_{\bar{v}}+\delta.$$

Thus, the comparison theorem holds that

$$V_{\bar{v}}\leqslant\frac{\delta}{2a_{\bar{v}}}+\left[V_{\bar{v}}(0)-\frac{\delta}{2a_{\bar{v}}}\right]\exp(-2a_{\bar{v}}t)\to\frac{\delta}{2a_{\bar{v}}}. \tag{18}$$

Therefore, we confirm the boundedness of $V_{\bar{v}}$. Thus, $e_{\bar{v}}$ is bounded, concluding the proof.

4.3 Boundedness of the agent-target distance-estimation error

Here, the boundedness of $\tilde{\rho}$ is proven. To guarantee PE, we rely on the following assumption to express the value range of δ.

Assumption 4. $0 < \delta < a_{\bar{v}}\alpha^2$.

Thereafter, the following lemma is obtained.

Lemma 7. Based on Conjecture 1, Assumptions 2–4, (1), and (16), it follows that $\bar{v}$ exhibits a positive lower bound after some time.

Proof. From Assumption 4, we confirm that there exist $\varepsilon_1, \varepsilon_2 \in \mathbb{R}_+$ satisfying $(\alpha-\varepsilon_1)^2 - 2\varepsilon_2 > 0$ such that $0 < \delta \leqslant a_{\bar{v}}[(\alpha-\varepsilon_1)^2 - 2\varepsilon_2]$. Therefore, $\frac{\delta}{2a_{\bar{v}}} + \varepsilon_2 \leqslant \frac{1}{2}(\alpha-\varepsilon_1)^2$. From (18), we know there exists a certain time t_0 such that $V_{\bar{v}} \leqslant \frac{\delta}{2a_{\bar{v}}} + \varepsilon_2$ for $t \geqslant t_0$. Thus, $V_{\bar{v}} = \frac{1}{2}e_{\bar{v}}^2 \leqslant \frac{1}{2}(\alpha-\varepsilon_1)^2$ for $t \geqslant t_0$. Therefore, we obtain $|e_{\bar{v}}| = |\bar{v}-\alpha| \leqslant \alpha - \varepsilon_1$. Hence, we know $\bar{v} \geqslant \varepsilon_1$ for $t \geqslant t_0$. This concludes the proof.

Proposition 2 (See [1])**.** Assuming the coefficient matrix, $A(t) \in \mathbb{R}^{n\times n}$, is continuous for all $t \in \mathbb{R}_{\geqslant 0}$, and constants $a, b \in \mathbb{R}_+$ exist such that for every solution of the homogeneous differential equation $\dot{z}(t) = A(t)z(t)$, where $z(t) \in \mathbb{R}^n$, we obtain $\|z(t)\| \leqslant b\|z(t_0)\|\exp(-a(t-t_0))$ for $0 \leqslant t_0 < t < \infty$. Therefore, for each $h(t)$ that is bounded and continuous on $\mathbb{R}_{\geqslant 0}$, every solution of the nonhomogeneous equation

$$\dot{z}(t) = A(t)z(t) + h(t), \quad z(t_0) = 0$$

is also bounded for $t \in \mathbb{R}_{\geqslant 0}$. Particularly, if $\|h(t)\| \leqslant K_h < \infty$, it follows that the solution of the perturbed system satisfies $\|z(t)\| \leqslant \frac{bK_h}{a} + \left(b\|z(t_0)\| - \frac{bK_h}{a}\right)\exp(-a(t-t_0))$.

Lemma 8. Under Conjecture 1, Assumptions 2–4, (1), and (16), the boundedness of $\tilde{\boldsymbol{x}}$ is confirmed.

Proof. Based on Lemma 7, we confirm that $\bar{\boldsymbol{\varphi}}$ satisfies the PE condition in the moving-target case. For any $\boldsymbol{z}(t) \in \mathbb{R}^2$, Proposition 1 ensures that the solution to the differential equation, $\dot{\boldsymbol{z}} = -k\bar{\boldsymbol{\varphi}}\bar{\boldsymbol{\varphi}}^{\mathrm{T}}\boldsymbol{z}$, which represents the corresponding homogeneous equation (2), converges exponentially to zero. Consequently, by applying Proposition 2, we confirm the boundedness of $\tilde{\boldsymbol{x}}$, concluding the proof.

4.4 Boundedness of the agent-target distance error

In this subsection, we prove that e_ρ is bounded.

First, we validate the following assumption about a_ρ^1 and a_ρ^0.

Assumption 5. $a_\rho^1, a_\rho^0 \in \mathbb{R}_+$.

Afterward, the following lemma is obtained.

Lemma 9. Conjecture 1, Assumptions 2–5, (1), and (16) confirm the boundedness of e_ρ.

Proof. Lemma 6 and Conjecture 1 confirm the boundedness of ω. Further, Lemma 8 reveals the boundedness of $\tilde{\rho}$. Based on Assumption 2, we confirm the boundedness of g. Assumption 5 illustrates that g can be considered as the bounded input of a stable system. The observed input-state stability confirms the boundedness of e_ρ.

Finally, Lemmas 6–9 lead to the following theorem, which summarizes this section.

Theorem 2. Under Conjecture 1, Assumptions 3–5, (1), and (16), it follows that

(1) $e_{\bar{v}}$, e_ρ, and $\tilde{\boldsymbol{x}}$ are bounded;

(2) $\bar{v}$ exhibits a positive lower bound after some time.

Hence, Problem 2 is solved.

5 Simulation

In this section, three simulations are performed and analyzed. First, we present the results for the static target case, covering noiseless and noisy cases, followed by the results for the moving target case.

The common parameters shared across these three simulations are defined below. The initial position and velocity of the agent are set $\boldsymbol{y}(0) = [20, 3]^{\mathrm{T}}$, $\dot{\boldsymbol{y}}(0) = [0, 0]^{\mathrm{T}}$. The desired agent-target circling distance and relative tangential speed are $d = 6$ and $\alpha = 2$, respectively. The initial value and coefficient of (1) are $\hat{\boldsymbol{x}}(0) = [4, 6]^{\mathrm{T}}$ and $k = 0.5$, respectively. The controller parameters are $a_\rho^1 = 3$, $a_\rho^0 = 2$, and $a_{\bar{v}} = 8$.

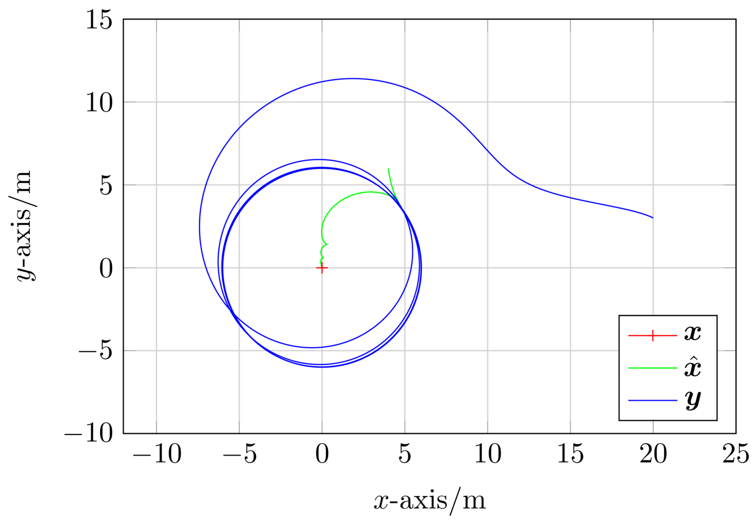

Figure 3 (Color online) Trajectories of agent's position $\boldsymbol{y}$ and target's estimated position $\hat{\boldsymbol{x}}$ in the static target case.

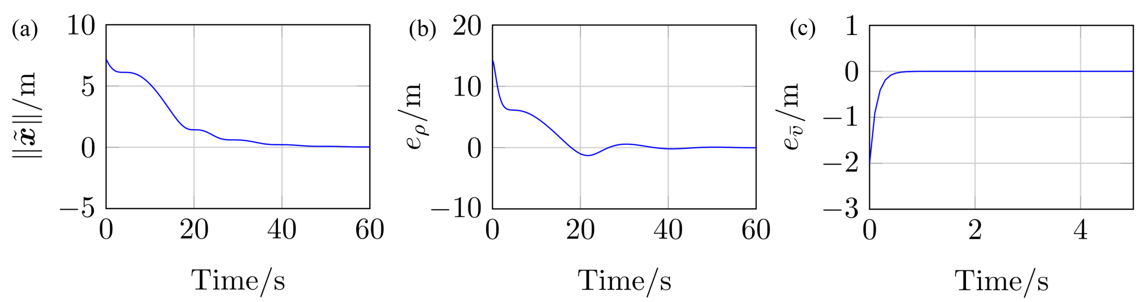

Figure 4 (Color online) (a) The agent-target distance estimation error's norm $\|\tilde{\boldsymbol{x}}\|$ in the static target case. (b) The agent-target distance error e_ρ in the static target case. (c) The agent-target relative tangential speed error $e_{\bar{v}}$ in the static target case.

5.1 Static target case

In the static target case, the target is set at position $\boldsymbol{x} = [0, 0]^{\mathrm{T}}$. In the following, both noiseless and noisy cases are simulated. The noiseless case denotes an ideal working environment, whereas the noisy case is a simulation for real working environments.

5.1.1 *Noiseless static target case*

For this case, the simulation results are shown in Figures 3 and 4. Figure 3 illustrates $\boldsymbol{x}$ as well as the trajectories of $\boldsymbol{y}$ and $\hat{\boldsymbol{x}}$, revealing that the agent approaches the desired orbit, whereas $\hat{\boldsymbol{x}}$ approaches its real position $\boldsymbol{x}$. Figure 4(a) shows the convergence of the estimator. Figures 4(b) and (c) show the convergence of the closed-loop error system (13).

The simulation result reveals that the agent performs the circumnavigation task.

5.1.2 *Noisy static target case*

To simulate a noisy operating environment, we introduce uncertainty to $\boldsymbol{x}$. Furthermore, each coordinate of $\boldsymbol{x}$ is perturbed by Gaussian white noise with a variance of 0.36. Consequently, the measured radial and tangential unit vectors $\boldsymbol{\varphi}$ and $\bar{\boldsymbol{\varphi}}$, respectively, are also perturbed.

The simulation results of the noisy static case are shown in Figures 5 and 6. As shown in Figure 5, besides $\boldsymbol{y}$ and $\hat{\boldsymbol{x}}$, the position of the noisy target is also plotted. These trajectories reveal that the estimator and the controller operate well in the noisy case. The variables $\|\tilde{\boldsymbol{x}}\|$, e_ρ, and $e_{\bar{v}}$ are shown in Figures 6(a)–(c), respectively.

These results reveal that the agent performs circumnavigation in the noisy static target case.

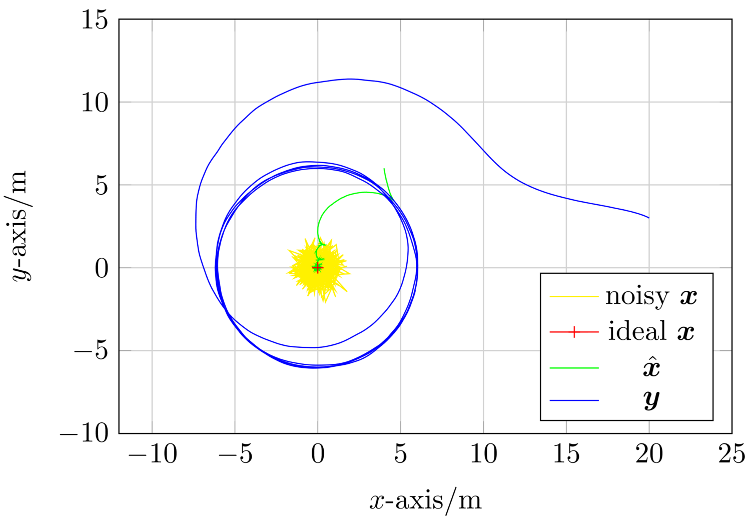

Figure 5 (Color online) Trajectories of noisy target's position, agent's position $\boldsymbol{y}$ and target's estimated position $\hat{\boldsymbol{x}}$ in the noisy static target case. "Noisy $\boldsymbol{x}$" denotes the target's position perturbed by Gaussian white noise with variance 0.36.

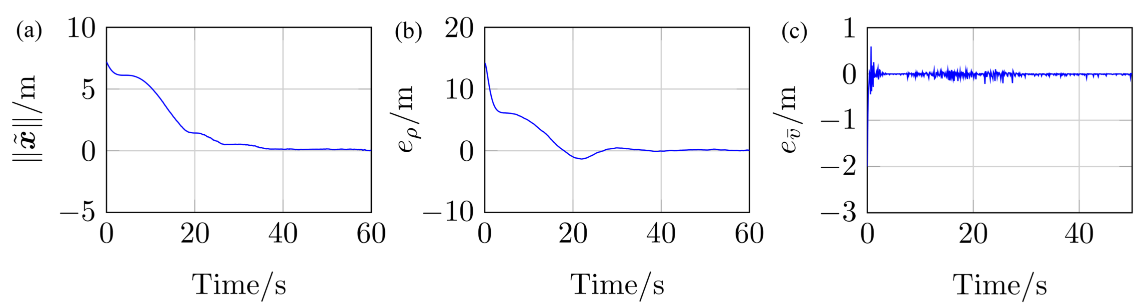

Figure 6 (Color online) (a) Agent-target distance estimation error's norm $\|\tilde{\boldsymbol{x}}\|$ in the noisy static target case. (b) Agent-target distance error e_ρ in the noisy static target case. (c) Agent-target relative tangential speed error $e_{\bar{v}}$ in the noisy static target case.

5.2 Moving target case

In this subsection, we present the simulation results for the moving target case. Since the moving target condition already introduces perturbation to the BOC system, we simply perform the noiseless simulation.

The following target trajectory is adopted from Deghat's classic study [1]:

$$\boldsymbol{x}(t) = \begin{bmatrix} 2 + 0.025t \\ 3 + \sin(0.025t) + 0.025t. \end{bmatrix}.$$

Therefore, we set $\varepsilon = 0.005$. Following Conjecture 1, we set $\rho_* = 2$. We select $\delta = 1 \leqslant a_{\bar{v}}\alpha^2 = 8 \times 2^2 = 32$ to satisfy Assumption 4. Given these parameters, the simulation results are illustrated in Figures 7 and 8. The trajectories of $\boldsymbol{x}$, $\boldsymbol{y}$, and $\hat{\boldsymbol{x}}$ are depicted in Figure 7. The evolution of ρ is shown in Figure 8(a), confirming that the relation $\rho \geqslant \rho_* = 2$ in Conjecture 1 is satisfied throughout the entire simulation. Furthermore, $\|\tilde{\boldsymbol{x}}\|$, e_ρ, and $e_{\bar{v}}$ are depicted in Figures 8(b)–(d), respectively.

These figures conclude that the circumnavigation task is executed by the agent when the target moves at a low speed.

6 Conclusion and future work

Research into the FAS-based BOC problem is currently in its early stages. The findings in [23], combined with the results of this study, indicate that the BOC problem can be effectively resolved using the FAS framework regardless of the specific estimator employed. Within this context, the error system defined in (13a) serves as a foundational result; it demonstrates that the convergence of the estimator directly ensures the stability of the controller.

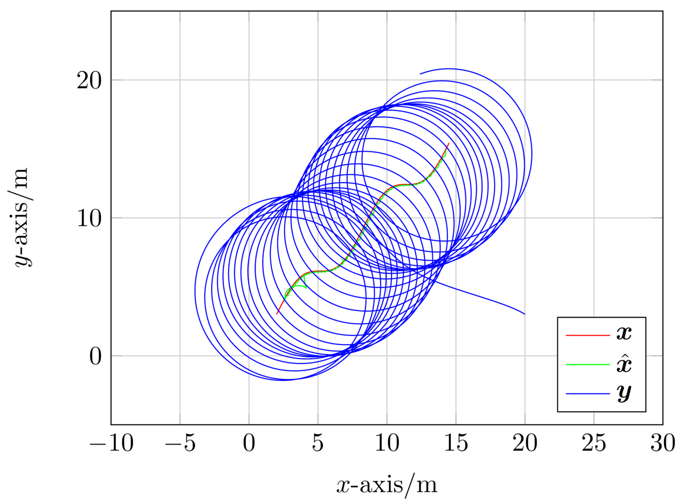

Figure 7 (Color online) Trajectories of agent's position $\boldsymbol{y}$, target's position $\boldsymbol{x}$ and target's estimated position $\hat{\boldsymbol{x}}$ in the moving target case.

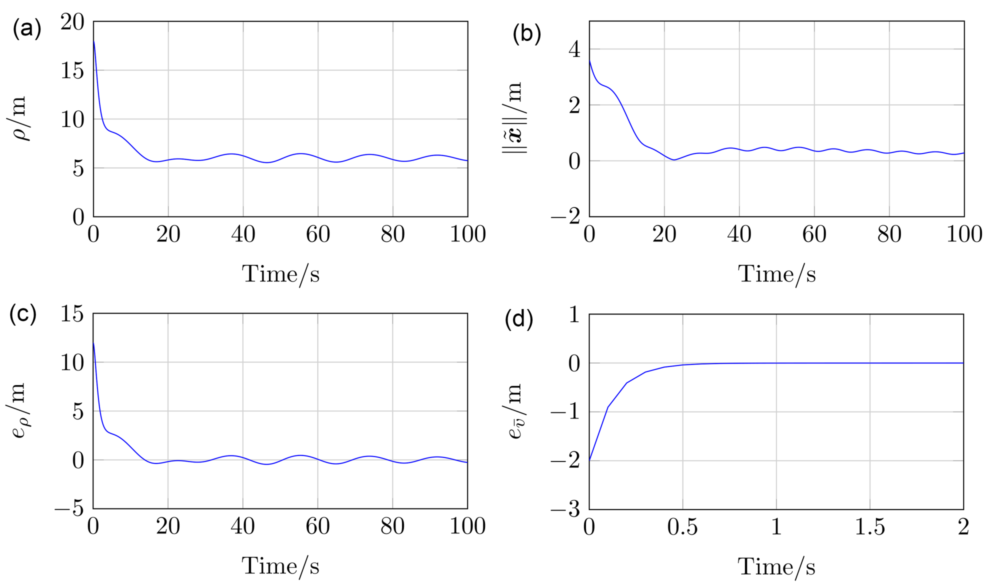

Figure 8 (Color online) (a) Agent-target distance ρ in the moving target case. (b) Agent-target distance estimation error's norm $\|\tilde{\boldsymbol{x}}\|$ in the moving target case. (c) Agent-target distance error e_ρ in the moving target case. (d) Agent-target relative tangential speed error $e_{\bar{v}}$ in the moving target case.

Thus far, the single-agent single-target acceleration-design BOC problem has been solved. However, there are still two limitations in resolving this problem.

(1) Angular velocity estimation problem: the determination of an estimator for ω.

(2) Safety problem: the study of the lower bound of ρ.

The assumption that ω is measurable and the conjecture that ρ_* is known in advance are not the perfect choices for addressing this BOC problem. Moreover, multi-agent or multi-target cases should also be considered in the future.

Acknowledgements This work was supported by National Natural Science Foundation of China (Grant No. 62188101), Guangdong Provincial Key Laboratory of Fully Actuated System Control Theory and Technology (Grant No. 2024B1212010002), Shenzhen Key Laboratory of Control Theory and Intelligent Systems (Grant No. ZDSYS20220330161800001), and Shenzhen Science and Technology Program (Grant No. KQTD20221101093557010).

References

1 Deghat M, Shames I, Anderson B D O, et al. Target localization and circumnavigation using bearing measurements in 2D. In: Proceedings of the 49th IEEE Conference on Decision and Control (CDC), 2010. 334–339

2 Deghat M, Davis E, See T, et al. Target localization and circumnavigation by a non-holonomic robot. In: Proceedings of the 2012 IEEE/RSJ International Conference on Intelligent Robots and Systems, 2012. 1227–1232

3 Deghat M, Shames I, Anderson B D O, et al. Localization and circumnavigation of a slowly moving target using bearing measurements. IEEE Trans Automat Control, 2014, 59: 2362–2374

4 Deghat M, Xia L, Anderson B D O, et al. Multi-target localization and circumnavigation by a single agent using bearing measurements. Int J Robust Nonlinear Control, 2015, 25: 2362–2374
5 Zheng R, Lin Z, Fu M, et al. Distributed control for uniform circumnavigation of ring-coupled unicycles. Automatica, 2015, 53: 23–29
6 Zheng R, Liu Y, Sun D. Enclosing a target by nonholonomic mobile robots with bearing-only measurements. Automatica, 2015, 53: 400–407
7 Li R, Shi Y, Song Y. Localization and circumnavigation of multiple agents along an unknown target based on bearing-only measurement: a three dimensional solution. Automatica, 2018, 94: 18–25
8 Bao Y, Shi Y, Li R, et al. Circling over a target based on bearing-only measurement. In: Proceedings of the 37th Chinese Control Conference (CCC), 2018. 7136–7140
9 Yu X, Liu L, Feng G. Distributed circular formation control of nonholonomic vehicles without direct distance measurements. IEEE Trans Automat Contr, 2018, 63: 2730–2737
10 Li R, Shi Y J, Wu X Q, et al. Safe-circumnavigation of one single agent around a group of targets with only bearing information. J Franklin Institute, 2019, 356: 11546–11560
11 Qi G Q, Li Y Y, Sheng A D. Virtual intersecting location based UAV circumnavigation and bearings-only target-tracking techniques. Inf Sci, 2019, 505: 571–585
12 Yu Y, Li Z, Wang X, et al. Bearing-only circumnavigation control of the multi-agent system around a moving target. IET Control Theory Appl, 2019, 13: 2747–2757
13 Cao S, Li R, Shi Y, et al. A low-cost estimator for target localization and circumnavigation using bearing measurements. J Franklin Institute, 2020, 357: 9654–9672
14 Yang Z, Zhu S, Chen C, et al. Entrapping a target in an arbitrarily shaped orbit by a single robot using bearing measurements. Automatica, 2020, 113: 108805
15 Dou L, Song C, Wang X, et al. Target localization and enclosing control for networked mobile agents with bearing measurements. Automatica, 2020, 118: 109022
16 Cao S, Li R, Shi Y, et al. Safe convex-circumnavigation of one agent around multiple targets using bearing-only measurements. Automatica, 2021, 134: 119934
17 Ma Y, Shi Y, Li R, et al. The distributed localization and circumnavigation of multiple targets based on bearing-only measurement in three-dimensional. In: Proceedings of the 2021 China Automation Congress (CAC), 2021. 8223–8228
18 Wang L, Zou Y, Meng Z. Stationary target localization and circumnavigation by a non-holonomic differentially driven mobile robot: algorithms and experiments. Int J Robust Nonlinear, 2021, 31: 2061–2081
19 Zou Y, Wang L, Meng Z. Distributed localization and circumnavigation algorithms for a multiagent system with persistent and intermittent bearing measurements. IEEE Trans Contr Syst Technol, 2021, 29: 2092–2101
20 Yue X, Shao X, Zhang W. Elliptical encircling of quadrotors for a dynamic target subject to aperiodic signals updating. IEEE Trans Intell Trans Syst, 2022, 23: 14375–14388
21 Wang W, Chen X, Jia J, et al. Target localization and encirclement control for multi-UAVs with limited information. IET Control Theory Appl, 2022, 16: 1396–1404
22 Zou Y, Yang W, He W, et al. Coordinate-free distributed localization and circumnavigation for nonholonomic vehicles without position information. IEEE ASME Trans Mechatron, 2022, 27: 2523–2534
23 Cao S, Duan G. Bearing-only circumnavigation based on fully actuated system approach. In: Proceedings of the 2nd Conference on Fully Actuated System Theory and Applications (FASTA), 2023. 361–366
24 Ma Z, Li Y, Qi G, et al. Finite-time distributed localization and multi-orbit circumnavigation with bearing-only measurements. J Franklin Institute, 2023, 360: 6712–6735
25 Wang C, Shi Y, Li R. Achieving safe minimum circle circumnavigation around multiple targets: a dynamic compensation approach. Int J Syst Sci, 2024, 55: 2980–2995
26 Zhou Z, Hu J, Chen B, et al. Target tracking and circumnavigation control for multi-unmanned aerial vehicle systems using bearing measurements. Actuators, 2024, 13: 323
27 Duan G. High-order system approaches: I. Fully-actuated systems and parametric designs (in Chinese). Acta Automat Sinica, 2020, 46: 1333–1345
28 Duan G. High-order fully actuated system approaches: Part I. Models and basic procedure. Int J Syst Sci, 2021, 52: 422–435
29 Cui K X, Duan G R, Hou M Z. Discrete-time model reference tracking control for a class of combined spacecraft: a high-order fully actuated system approach. IEEE Trans Automat Sci Eng, 2024, 21: 6966–6977
30 Duan G. High-order fully actuated system approaches: part III. Robust control and high-order backstepping. Int J Syst Sci, 2021, 52: 952–971
31 Duan G. High-order fully actuated system approaches: part VII. Controllability, stabilisability and parametric designs. Int J Syst Sci, 2021, 52: 3091–3114